

Fully-Integrated CMOS-Compatible Q-Switched Laser at 1.9 μm Using Thulium-Doped Al₂O₃

Patrick T. Callahan¹, Katia Shtyrkova¹, Nanxi Li^{1,2}, E. Salih Magden¹, Purnawirman¹, Christopher Baiocco³, Douglas Coolbaugh³, Erich P. Ippen¹, Michael R. Watts¹, and Franz X. Kärtner^{1,4,5}

¹Research Laboratory of Electronics, Massachusetts Institute of Technology, 50 Vassar St. Cambridge, MA 02139, USA

²School of Engineering and Applied Sciences, Harvard University, 29 Oxford St. Cambridge, MA 02139, USA

³College of Nanoscale Science and Engineering, State University of New York, 257 Fuller Rd. Albany, NY 12203, USA

⁴Department of Physics, University of Hamburg, Notkestraße 85, Hamburg 22607, Germany

⁵Center for Free-Electron Laser Science, Deutsches Elektron-Synchrotron, Luruper Chaussee 149, Hamburg 22761, Germany

Author e-mail address: pcallahn@mit.edu

Abstract: A fully-integrated Q-switched laser is demonstrated at 1.9 μm using thulium-doped aluminum oxide waveguides, with the potential for achieving an on-chip passively mode-locked laser. All components of the laser are fabricated in a CMOS-compatible silicon photonics process.

OCIS codes: (140.4050) Mode-locked lasers; (140.3540) Q-switched lasers; (130.3120) Integrated optics devices.

1. Introduction

Mode-locked lasers (MLLs) have many important applications, including low-noise photonic oscillators, frequency combs and drive photonic analog-to-digital conversion. As silicon photonics technology continues to develop, there is increasing interest in fabricating mode-locked lasers on-chip [1-3]. In particular, the ability to fabricate devices that can be co-integrated with CMOS electronics is highly desirable in order to enable inexpensive mass production of systems with low size, weight and power. In the context of on-chip frequency combs, MLL operation in the 2 μm wavelength range is advantageous for generating octave-spanning supercontinuum within the transparency window of silicon [4-6]. In this paper we present progress towards a fully-integrated passively-mode-locked laser operating at 1.9 μm , which exhibits Q-switched pulsing when pumped at 1.6 μm .

2. Laser Design and Fabrication

The laser cavity consists of a 13-cm spiral gain waveguide, a double-chirped Bragg grating for dispersion compensation similar to that described in [7], and a nonlinear interferometer (NLI) that acts as an artificial saturable absorber as well as the output coupler. The principle of operation and characteristics of the NLI are described in detail in [8]. The gain waveguide consists of an inverted ridge structure, with a segmented silicon nitride slab forming the guiding layer underneath a thin film of thulium-doped Al₂O₃. We have used similar waveguide designs in our group to achieve high-power efficient DFB and DBR lasers operating around 1.9 μm [9]. A cross-section of the waveguide is shown in Figure 1(a), and a schematic of the full laser cavity is shown in Figure 1(c). All the components in the cavity are integrated on-chip and were fabricated in a 300-mm CMOS foundry, using PECVD to grow the nitride layer and optical immersion lithography to pattern the various waveguide structures. We then deposit a layer of the Tm³⁺:Al₂O₃ gain material using reactive co-sputtering.

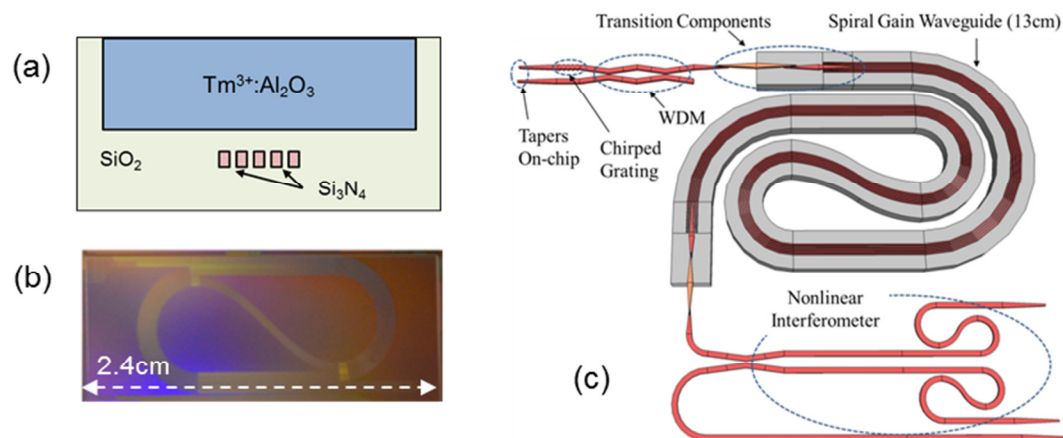


Fig. 1. (a) Cross-section of gain waveguide. (b) Photograph of spiral laser structure. (c) Schematic of laser cavity with components labeled.

3. Experimental Results

A schematic of the experimental setup is shown in Figure 2. To test the performance of the laser structures, we use an L-band EDFA to amplify the 1614-nm pump laser. The pump passes through a polarization controller and is coupled onto the chip using a lensed fiber, which is mode-matched to a nitride waveguide at the chip facet to minimize coupling losses. The laser output is then collected with another lensed fiber from the output port of the NLI, and measured with an optical spectrum analyzer. The time-domain behavior and RF spectrum are also measured from the output of a photodiode.

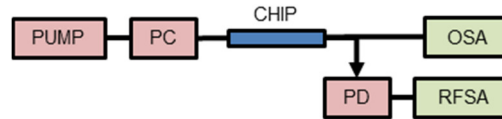


Fig. 2. Schematic of experimental setup. Abbreviations are as follows: PC – polarization controller, PD – photodiode, OSA – optical spectrum analyzer, RFSA – RF spectrum analyzer.

The output spectrum of the laser is shown in Figure 3(a), for various different input pump power levels. As the pump power is increased, the laser first exhibits multimode CW operation before then beginning to emit Q-switched pulses, as shown in Figure 3(b). As the pump power is increased to its maximum – approximately 1W of on-chip power – the spectrum begins to broaden considerably, which suggests operation very close to the threshold for stable mode-locking.

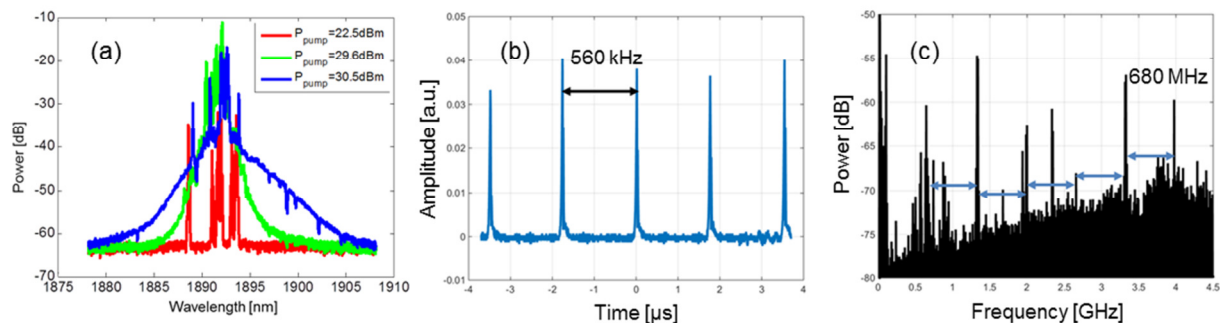


Fig. 3. (a) Optical spectrum of laser output for various input pump powers. (b) Time-domain behavior of Q-switched pulses with a pulse repetition rate of 560 kHz. (c) RF spectrum of detected pulses showing harmonics of the cavity repetition rate of 680 MHz.

4. Conclusion

We have demonstrated Q-switched pulsing at $1.9\mu\text{m}$ in a fully-integrated thulium-doped laser with on-chip dispersion compensation and artificial saturable absorbers, fabricated in a CMOS-compatible silicon photonics platform. The broadening of the output spectrum at high pump powers suggests that the structures are very close to the mode-locking threshold. Future work will focus on increasing the intracavity power to achieve passive mode-locking on chip.

Acknowledgements

This work was supported under the DARPA DODOS project by Robert Lutwak, contract number HR0011-15-C-0056.

References

- [1] H. Byun, et al., "Integrated Low-Jitter 400-MHz femtosecond waveguide laser," *IEEE PTL*, vol. 21, no. 12, pp. 763-765. (2009)
- [2] C. Sorace-Agaskar, et al., "Integrated mode-locked lasers in a silicon photonics platform," *CLEO: 2015 OSA Technical Digest*, (Optical Society of America, 2015), paper SM2I.5.
- [3] V. Corral, et al., "Optical frequency comb generator based on a monolithically integrated passive mode-locked ring laser with a Mach-Zehnder interferometer," *Opt. Lett.*, vol. 41, no. 9, pp. 1937-1940. (2016)
- [4] R.K.W. Lau, et al., "Octave-spanning mid-infrared supercontinuum generation in silicon nanowaveguides," *Opt. Lett.*, vol. 39, no.15, pp.4518-4521. (2014)
- [5] N. Singh, et al. "Midinfrared supercontinuum generation from 2 to $6\mu\text{m}$ in a silicon nanowire," *Optica* vol. 2, pp. 797-802 (2015).
- [6] N. Singh, et al., "Octave spanning supercontinuum generation in silicon from $1.1\mu\text{m}$ to beyond $2.4\mu\text{m}$," submitted to *CLEO 2017*.
- [7] P. T. Callahan, et al., "Double-chirped Bragg gratings in a silicon nitride waveguide," *CLEO: 2016 OSA Technical Digest*, (Optical Society of America, 2016), paper SF1E.7.
- [8] K. Shtyrkova, P.T. Callahan, E.P. Ippen and F.X. Kärtner, "Fully-integrated artificial saturable absorber based on Kerr nonlinearity in silicon nitride," submitted to *CLEO 2017*.
- [9] N. Li, et al., "High-power thulium lasers on a silicon photonics platform," accepted for publication in *Opt. Lett.* 2017.